

University of Minnesota
ST. ANTHONY FALLS HYDRAULIC LABORATORY

Project Report No. 172

AN EXPERIMENTAL INVESTIGATION OF THE EFFECT OF DRAG REDUCING
POLYMER ADDITIVES ON SURFACE PRESSURE FLUCTUATIONS
ON BODIES OF REVOLUTION WITH ROUGH SURFACES
MOVING THROUGH WATER

by

Edward Silberman

This research was carried out under the Naval Sea Systems
Command General Hydromechanics Research Program administered
by the David W. Taylor Naval Ship Research and Development
Center (1505) under Office of Naval Research
Contract N00014-77-C-0356.

May 1978
Minneapolis, Minnesota

Foreward

This research was funded under the General Hydrodynamics Research Program of the David W. Taylor Naval Ship Research and Development Center, Contract N00014-77-C-0356. The contract was effective May 1, 1977 and terminated April 30, 1978. This is the final technical report on this one year contract and describes and summarizes all of the work that was done. The original proposal contemplated more than one year of work and the task is admittedly unfinished. However, it has been possible to draw several potentially useful conclusions.

The research was conducted under the supervision of the author, Professor Edward Silberman. Technical assistance was provided by Jeff Ferguson, Associate Scientist, and Jerry Moore, Research Assistant at the St. Anthony Falls Hydraulic Laboratory. Dr. John Killen, Research Associate at the Laboratory, consulted on the work and critically reviewed the final report. The help of these persons as well as that of the editorial and clerical staff, shop personnel, and other assistants at the Laboratory is gratefully acknowledged.

ABSTRACT

A sound detector in the surface of a moving body receives not only sound signals radiated from a distant source but also detects pressure fluctuations originating in the turbulent boundary layer of the fluid surrounding the body. The purpose of the present work was to assess the magnitude of the surface pressure fluctuations on a body moving in water and in water with polymer additive under nearly zero pressure gradient conditions. Measurements were made using a single transducer in the surface of an axi-symmetric body. Both smooth and grit-roughened surfaces were used. Mean square pressure fluctuation amplitudes were measured as a function of frequency, non-dimensionalized, plotted, and compared with some results obtained by others in both water and air.

It was concluded that the addition of roughness to a smooth surface increases the amplitude at the peak of the spectrum and at all lower frequencies. Polymer additive in the water has just the opposite effect on a rough-surfaced body, decreasing the amplitude at the peak and at all lower frequencies, the reduction increasing monotonically with drag reduction. There was little or no effect at high frequencies attributable to either roughness or polymer additive, but it must be noted that the transducer used was too large to obtain a true measure of amplitude at the highest frequencies. The peak of the spectrum in water appears to have a somewhat higher amplitude than it does in air.

AN EXPERIMENTAL INVESTIGATION OF THE EFFECT OF DRAG REDUCING
POLYMER ADDITIVES ON SURFACE PRESSURE FLUCTUATIONS
ON BODIES OF REVOLUTION WITH ROUGH SURFACES
MOVING THROUGH WATER

Introduction

The turbulent boundary layer associated with the flow of fluid over a solid surface has a unique dynamic structure; an interesting aspect of this structure is the surface pressure fluctuations [1, 2, 3]* which accompany the flow. Those fluctuations do not radiate sound so that they can only be sensed with a very small transducer mounted in the boundary surface. Such a transducer, though, cannot distinguish between these surface pressure fluctuations and sound pressure radiated from outside the boundary layer. Roughness on a flow surface intensifies the pressure fluctuations [3, 4, 5].

It is well known that polymer additives in water tend to reduce surface pressure fluctuations from turbulent boundary layers [5, 6, 7, 8, 9] as well as to reduce drag. However, all of the previous measurements to examine noise reduction have been made on what might be called "fully developed" boundary layers, mostly thick layers. This report describes recent measurements made in a thin, developing boundary layer on a rough surface moving through tap water and tap water with polymer additive. The work was supported from May 1, 1977 to April 30, 1978 under contract N00014-77-C-0356 with the U.S. Naval Ship Research and Development Center.

*References on page 16.

Some Previous Experimental Work

Blake [3] summarized his own and some other measurements of pressure fluctuation spectra on smooth and rough surfaces moving through air at zero pressure gradient. Figures 1 to 4 are reproduced from his paper and show several forms of dimensionless plotting of data. In particular, there are two different sets of reference quantities--an outer set using U_∞ and δ^* and an inner set using U_τ and U_τ/ν or \bar{k}_g as velocity and length parameters, respectively. Here U_∞ is the free stream velocity, $U_\tau = (\tau_w/\rho)^{1/2}$ is the shear velocity where τ_w is wall shear stress, δ^* is the boundary layer displacement thickness, ν is the kinematic viscosity and ρ the density of the fluid, and \bar{k}_g is an equivalent roughness height. Also ω is radian frequency, $q = 1/2 \rho U_\infty^2$ is the dynamic head of the free stream, and $\Phi(\omega)$ is the mean square pressure per radian. It may be noted that measurements from two flow situations will plot differently relative to each other when plotted on inner coordinates than when plotted on outer coordinates if the Reynolds numbers and/or roughness are different in the two cases. However, for completely rough surfaces, data curves should be transformed nearly similarly between the two forms of plotting.

Blake argues that the outer set of coordinates is appropriate to the lower frequency (presumably larger) eddy or wave structure which moves along at nearly free-stream speed; the inner set applies to the high frequency part of the spectrum wherein eddies or waves move at the lower speeds characteristic of the region where wall turbulence is produced. The larger eddies or waves may be associated with the normal growth of the boundary layer or may be convected or radiated from other sources. (It may be noted in passing that low frequency pressure fluctuations originate not only from the large-eddy structure but also from small eddies generated infrequently [2]. However, it would be expected that the latter source would contribute considerably less to the mean square pressure than the former.)

There are problems in making low frequency measurements because of the various extraneous sources that may generate large eddies. In wind tunnels, acoustic fluctuations have caused trouble and need to be filtered out [1, 10, 11]. To illustrate the problem, some data taken by Hodgson on the wing of a full-scale glider, presumably without low-frequency filtering, and plotted

by Willmarth [1] has been reproduced on Fig. 2 for comparison with Blake's wind tunnel data. The difference seen in Fig. 1 between Blake's and Schloemer's data at low frequency may possibly also be attributed to differences in filtering. At high frequencies, Blake's data in Fig. 1 show clearly the importance of using small transducer surfaces to avoid averaging out the short-duration, large-amplitude pressure fluctuations [1].

In water, the data trends from two previous sets of measurements on smooth surfaces are reproduced as spectra in Fig. 5. The same outer coordinate scales have been used as were used in Fig. 1. The data by Nisewanger and Sperling [2] were obtained using a torpedo-shaped body with tailfins, rising by buoyancy in a fresh water lake. The data are for a station far enough back from the nose that the pressure gradient is approximately zero. It was determined in the experiments that the transducer was not sensitive to accelerative forces. There was no separate filtering of the low frequency signals in these measurements. It is possible for surface waves to produce pressure fluctuations at very low frequencies (2 Hz corresponds to a 1.28 ft wave length), but these will likely be below transducer and amplifier cutoffs. The mean square pressure level for these data at low frequencies is clearly several decibels larger than are the data for air shown in Fig. 1 while, on the other hand, the mean square pressure level at high frequencies is even more clearly very small compared to the air data shown in Fig. 1. It is believed that the latter difference may be explained by the relatively large size of the transducer used to obtain the water data but the difference at low frequencies is not so readily explained.

The water data reported by Greshilov, et al. [5] are summarized by a broken line in Fig. 5. These data were obtained on one wall of a 2 cm high closed channel of aspect ratio 3.5; there was fully developed flow in the channel. It is not known whether any filtering was done in taking the data. The authors non-dimensionalized their data using the mean velocity in the channel for reference velocity and the mean channel height for reference length. In order to plot the data on Fig. 5, δ^* and centerline velocity (assumed to be U_∞) were obtained from the given data using power laws for the velocity profiles for fully-developed channel flow. Several power laws-- $1/7$, $1/8$, $1/9$ --were tried but they produce data trends so close to each other that only the results using the $1/8$ power are plotted. The differences between these two sets of water data can probably be attributed to the different

boundary conditions and to uncertainties in reducing the Greshilov, et al data from plotted points. However, the latter data do seem to support the disagreement at low frequencies between the Nisewanger and Sperling water data and Blake's air data.

Greshilov, et al [5] also obtained data with rough surfaces in their channel both without and with polymer additives in the water. One of their figures is reproduced in Fig. 6 in dimensional form (amplitude is averaged over 1/3 octave bands); the roughness used for this case is grit roughness of about 0.4 mm height. There is not enough information in the paper to make Fig. 6 dimensionless in such a way as to compare with Figs. 1 to 4.

Experimental Program

The current research program is being conducted with a buoyancy propelled, axi-symmetric body, rising along a guide cable in a vertical standpipe [12] as sketched in Fig. 7. The body is somewhat like the Nisewanger and Sperling test body [2] except that no tail fins are required. It is formed from a theoretical half-body nose faired into a cylindrical center portion with a conical tail and is sketched in Fig. 8. The standpipe has an inside diameter of 1.06 m and a working depth of about 24 m. The maximum buoyant force on the body is 342.9N. Lead weights placed within the body are used to reduce the buoyant force. For the present work, two different buoyant forces were used, 342.9N and 222.8N. (Although the interior of the body remains dry most of the time, water leakage has been found on occasion. The force has been reduced thereby as much as 5N, but lacking a measurement of leakage at the time of each experiment, the nominal forces have been used in computations.) At terminal velocity these buoyant forces are equal to body drag.

At a location 57 cm back of the nose as shown in Fig. 8, a hole of about 12 mm diameter has been provided in the body for mounting hydrophones or other transducers. The hole is in a zone of nearly zero pressure gradient. For the current work, a single pressure sensitive transducer has been installed at this place to measure surface pressure fluctuations. The transducer was built at the U.S. Navy David Taylor Ship Research and Development Center a number of years ago and was described by Franz [13]. It is a crystal type with a 3.1 mm diameter sensing area. In experiments conducted several years ago it was determined that when this transducer is mounted in the test

body, the noise level attributable to acceleration or other external sources is many dB below the signal to be measured [12, Fig. 10]. The transducer was calibrated against a USRD type H23 crystal hydrophone obtained on loan from the Underwater Sound Reference Division, U.S. Naval Research Laboratory, Orlando. After preamplification, the signal from the transducer is fed to the surface via a trailing cable where it is further amplified or attenuated, as necessary, and recorded on an instrumentation magnetic tape recorder. The signal is split into high and low frequency components, which are recorded on separate channels of the recorder in order to increase the effective dynamic range of the recorder.

As seen in Fig. 7, a taut guide cable runs up the center of the standpipe. The cable is steel. Insulated wire coils have been mounted on the cable at 20 cm intervals. The entire assembly is covered by a plastic sheath to protect the coils and to provide a smooth exterior surface to guide the body. A magnet in the nose of the body produces a small electrical signal as it passes over the coils; this is used to measure the speed and position of the body. The velocity signal is recorded simultaneously with the pressure data signal. A typical record from the tape recorder has been reproduced on a strip chart recorder and is shown in Fig. 9.

In addition to the body transducer, the USRD type H23 hydrophone has been mounted in the standpipe, attached to the pipe wall, to attempt to measure radiated sound. It is located 40 cm from the central steel cable (13 cm from the wall) and about 5.5 to 6 m below the water surface. The signal from this hydrophone is recorded in the same manner as that from the surface pressure transducer. A typical record is shown in Fig. 10. (In connection with Fig. 10, the potential flow pressure field for a half body in infinite fluid has been used to calculate the position of the nose of the body when the pressure maximum occurs at 40 cm from its axis. This distance is 23.4 cm along the axis as indicated on Fig. 10. Likewise, the position of minimum pressure has been calculated and lies 34.2 cm behind the nose making the total distance between maximum and minimum 57.6 cm; this seems to agree exactly with the maximum and minimum pressures marked at A and B, respectively on Fig. 10. The calculated maximum and minimum pressures are $0.0139 \frac{\rho U^2}{2}$ at A and $-0.0142 \frac{\rho U^2}{2}$ at B. The amplitude scale in Fig. 10 was not calibrated but the minimum pressure does not appear

to be sufficiently negative when compared with the recorded maximum and minimum pressures; this may be due to the failure to correct for the presence of the wall or to the bleeding of the pressure from the crystal transducer.)

The tape recorded pressure data are processed with an analog, constant bandwidth, spectrum analyzer. Central frequencies for analysis are 20, 30, 40, 50, 60, 80, 100, 150 (sometimes), 200, 300, 400, 500, 600, and 800 Hz and 1, 1.5, 2, 3, 4, 5, 6, 8, 10, 12, 15, and 20 kHz. The bandwidth is always less than 10 percent of the central frequency except that the minimum width is 10 cycles. The data produced by the analyzer are then normalized to a pressure squared per radian bandwidth format. These data may be plotted versus frequency to obtain a spectrum and this may be non-dimensionalized in several ways as discussed previously.

Table 1 shows the conditions under which experimental measurements were obtained. Each experiment at given conditions consisted of 3 or more runs. The velocities shown in Table 1 have been corrected for blockage; correction requires multiplying the measured velocity by 1.06 [14]. Velocity was measured over the last 0.5 sec or less of motion before the body hit the arresting year, shorter times being used when terminal velocity was not reached during the last half second. This was the case at velocities over 11 mps, but the tabulated values are still within a few percent of the correct terminal velocity.

Roughness, when used, was the same in every case. Glass beads, 0.46 mm diameter, were fastened to the body surface using a laquer coating. A surplus of beads was applied to the surface and the excess beads were then brushed off. A closely-spaced grit roughness was obtained in this way. Figure 11 shows a detail of the appearance of the rough surface. Roughness covered the body from about 5 cm back of the nose to about 10 cm beyond the transducer location; the remainder of the body was in its original smooth condition. A clear space of about 12 mm diameter was maintained around the transducer. Earlier work [6, Fig. 19] indicated that this would not significantly influence the transducer response.

Table 1 - Experimental Runs

<u>Series</u>	<u>Drag</u>	<u>Expt</u>	<u>Surface Condition</u>	<u>Total Drag Coefficient Reduction Due to Polyox Addition</u>	<u>Terminal Velocity</u>
	N			%	$U_{\infty}, m/s$
1	342.9	1A	Smooth	0	10.8
		1B	Rough	0	8.5
		1C	Rough	40	11.0
		1D	Rough	55	12.7
		2A	Smooth	0	8.06
2	222.8	2B	Rough	0	6.57
		2C	Rough	34	8.06
		2D	Rough	40	8.5

Experimental Results

Figure 12 is a dimensionless plot of the mean square surface pressure fluctuation data obtained on the smooth body at two different Reynolds numbers. Outer layer parameters have been used for determining coordinates. The two sets of data agree with each other fairly well except at low frequencies. The Nisewanger and Sperling [2] and Gershilov, et al [5] data trends are also reproduced in this figure and the comparison with the present data is seen to be reasonably good except for the low frequency data at the lower velocity.

The same data used in Fig. 12 have been replotted in Fig. 13 using inner layer parameters. The trend of Blake's [3] data taken in air is represented by a solid line in this figure. Discrepancies between the present data and Blake's in the high frequency range are probably due to transducer size as was demonstrated by Blake for air. The disagreement in the low frequency range near the peak of the spectrum seems to be of the same order as occurs using outer variables as was seen in Fig. 5.

In order to non-dimensionalize the data for use in Figs. 12 and 13, it was necessary to estimate the boundary layer parameters. Calculations

have been made for δ^* and U_r at the transducer location for the smooth body following Granville [15]. In the boundary layer calculations, surface pressure distributions were obtained from potential flow calculations made for an identical body (except for a slightly different tail angle) in infinite fluid [16] using the U_∞ values cited in Table 1. The interesting boundary layer parameters are given in Table 2.

Table 2 - Boundary Layer Parameters

<u>Expt</u>	<u>U_∞</u> m/s	<u>$Re_L \times 10^6$</u>	<u>$Re_{x_{trans}} \times 10^6$</u>	<u>θ</u> mm	<u>δ^*</u> mm	<u>U_r</u> m/s	<u>$c_f \times 10^3$</u>	<u>c_F (est)</u> <u>$\times 10^3$</u>	<u>c_D (meas)</u> <u>$\times 10^3$</u>
1A	10.8	14.8	1.84	1.01*	1.4#	0.41*	2.79*	2.43	4.74
1B	8.5	11.7				0.50#	6.81#	5.34	7.65
1C	11.0	15.1				0.42#	2.87#	2.26	4.57
1D	12.7	17.4				0.36#	1.58#	1.12	3.43
2A	8.06	12.8	1.62	1.02*	1.4#	0.31*	2.87*	3.22	5.53
2B	6.57	10.9				0.36#	5.91#	6.02	8.33
2C	8.06	13.95				0.33#	3.30#	3.22	5.53
2D	8.5	13.75				0.31#	2.62#	2.66	4.97

*Calculated

#Rough estimate

The points plotted in Figs 12 and 13 were obtained using saturated tap water in the tests. It was thought at one time that the anomalous rise in the spectrum for the highest 3 frequencies (12, 15, and 20 kHz) might be attributable to cavitation in the boundary layer or to small entrained bubbles in the water. Hence, tests were also conducted with partially deaerated tap water to test this hypothesis. The data points were almost identical with those shown in Figs 12 and 13; it is assumed, therefore, that the postulated effects do not exist. It was discovered subsequently that the anomalous rise at high frequencies might probably be due to the limited dynamic range of the tape recorder causing harmonics of lower frequency

signals to be recorded as part of the high frequency signals. It was thought that this problem had been corrected by splitting the signal into high and low frequency components which are recorded separately as previously explained, but subsequent measurements tend to show the same anomaly. Consequently data points obtained at 15 and 20kHz are not plotted on subsequent figures.

Non-dimensionalized data for the rough surface in tap water are shown for the two velocities in Fig. 14 using inner variables. Although the two sets of data agree quite well in general, there does seem to be a small systematic difference at dimensionless frequencies below 0.005. Trend lines for the smooth surface data from Fig. 13 are also shown in the figure. It appears that rough surfaces behave somewhat like smooth surfaces when data are non-dimensionalized in this manner, but there is a large increase in amplitude at low frequencies and some decrease at high frequencies.

The U_r values used for non-dimensionalizing the rough body data in Fig. 14, as well as in the subsequent figures, were not calculated directly but were estimated from the smooth body calculations knowing the total drag coefficient for each experiment. The estimate was made by subtracting the smooth body estimated friction drag from total drag to obtain a pressure drag and pressure drag coefficient. The pressure drag coefficient was then assumed to be constant for all other experiments with the same buoyant force. Thus, the skin friction drag for each test could be estimated; its distribution on the body was further estimated to obtain U_r at the transducer location. The estimate of U_r may easily be in error by 10 per cent or more because of this process. On Fig. 14, the shift in scale caused by a 10 per cent error in U_r is shown on both coordinates and similar information is given in Figs. 12, 13, and 16.

The rough surface data are replotted on inner coordinates using roughness height as a length parameter in Fig. 15. This figure is comparable to one of Blake's figures [3] reproduced as Fig. 4 herein; the data trend from Fig. 4 is reproduced in Fig. 15. Of course, the equivalent roughness height is not known for the present work and the glass bead diameter is used instead. It is believed that the present roughness is comparable to Blake's roughness that produced the lower branch of the curve in Figs. 4 and 15.

Figure 16 shows surface pressure fluctuation data obtained for the rough body with two different concentrations of Polyox added to the tap water in the standpipe. Since the measurement of Polyox concentration in the standpipe could not be obtained very accurately (it is not even certain that the mixture was entirely homogeneous), the effect of additive is expressed as a percentage of total drag coefficient reduction. The 3 or more consecutive runs for each experiment were made at intervals of about 1/2 hour; no evidence of polymer degradation (as would have been indicated by changes in terminal speed) was found during any of the experiments. The trend line for the rough surface data without additive in the water has been transcribed from Fig. 14 for comparison. High frequency spectra do not appear to be influenced but there is a progressive decrease in amplitude with increased drag reductions at low frequencies.

As previously noted, a fixed external transducer had been provided to measure radiated sound from the body. It was believed that a reverberant field might be established in the tank and that this could be detected by the non-directional hydrophone provided. However, analyses of the records obtained, such as in Fig. 10, do not show an effect that can be attributed to radiated sound and more work is needed before a useful record can be made. At 300 to 500 Hz and again at 10 to 20 kHz, there are some interesting pressure fluctuations on the transducer that appear to cover just the time span when the body boundary layer is turbulent. At all other frequencies, however, the fluctuations appear to exist in the water even when the body is not moving and do not appear to change their amplitudes when the body is moving.

Some Comments on the Experimental Results

There are several results that require comment. First, the general shapes of all the spectral curves (smooth and rough surfaces in water and rough surface in water with Polyox) appear to be similar to those obtained by others. Mean square pressure amplitude increases gradually with frequency at low frequencies reaching a peak at a dimensionless frequency $\omega \delta^* / U_\infty \approx 0.4$ or $\omega \nu / U_r^2 \approx 0.02$ (possibly less on rough surfaces) and then decreases at an increasing rate until at high frequencies the decrease is about 72dB per decade of frequency as indicated on Figs. 12 to 16.

Consider the high frequency part of the spectrum first. Comparing Fig. 12 with Fig. 1, Fig. 13 with Fig. 3, and Fig. 15 with Fig. 4, it appears that the

data obtained in water all have lower amplitudes than data obtained in air in this frequency range. As has already been pointed out, this is probably attributable to the large diameters of the transducers compared to boundary layer thicknesses as used in water. Blake [3] had already shown for air that larger relative transducer sizes caused a decrease in measured amplitude; Nisewanger and Sperling [2, Fig. 4] confirmed this for even larger transducers in water. There is no reason to doubt that the same explanation can be extended to the comparison between the present water data and air data. However, there is a need to make a further check of this effect with smaller transducers, especially on rough surfaces. Such a check is required not only to determine whether the explanation is correct but also to know whether interpretations regarding trends of data in the high frequency part of the spectrum can be based on data obtained with large transducers.

In spite of the question just raised about data interpretation, some comments will be made about the data in the high frequency part of the spectrum. The only justification for doing this is that the same transducer and electronic circuitry have been used for all experiments and there is a uniform decrease of about a 72dB per decade of frequency at the highest frequencies for all the data (which is also true for Blake's data in air as seen in Figs. 1 to 4). Comparing rough surfaces with smooth ones, then, Fig. 14 versus Fig. 13, it appears that the rough surface produces somewhat lower mean square pressure amplitude than the smooth surface at high frequencies. When Polyox is added to the water with a rough-surfaced body, Fig. 16 versus Fig. 14, the amplitude does not appear to change. In other words, even though the additive increases the velocity toward that of the smooth-surfaced body, it does not increase the pressure amplitude toward the smooth surface amplitude. It is unfortunate that the data of Gershilov, et al [5] displayed in Fig. 6 cannot be non-dimensionalized for comparison with the present data. The data with additive do show a decrease of about 72dB per decade of frequency just as the present data do at the highest frequencies but this is not true for the data in plain water.

All of the figures, 12 to 16, show an anomalous region just as the slope of the data trend becomes 72dB per decade. This looks suspiciously like a resonance phenomenon. The apparently high data points in each case are at 3,

4, or 5 kHz. On the other hand, there is a very definite reverse curve in the data trend at this place (which can also be seen to a small extent in the Nisewanger and Sperling data [2]) that does not appear in any air data. This region needs further study. The Laboratory has acquired new transducers of a different manufacture than those currently in use and the earliest work to be undertaken if this research is resumed will be concerned with better defining this region.

Looking now at the low frequency regions of the several spectra, there is some question as to how well the amplitudes are being measured at the lowest frequencies. The problem is that each run has very short duration at terminal velocity (one-half second or less). It would be especially useful to have correlation measurements between two adjacent transducers at the lowest frequencies to verify whether the higher or lower data trends appearing in Figs. 12 and 13 are correct. The air data seem to indicate that the higher plotted points are more to be expected, but the air data are contaminated by filtering.

Considering the region around the peaks of the spectrum there should be little question about the ability of the apparatus to obtain reasonable measurements. Comparing Fig. 12 with Fig. 1, Fig. 13 with Fig. 3 or even Fig. 15 with Fig. 4 (where the present roughness probably corresponds best to the D-L roughness of Fig. 4) it appears that the water data are consistently a few dB higher in amplitude than the air data. This is true not only for the present data but also for that of Nisewanger and Sperling [2] and of Gershilov, et al [5]. It is believed that the difference is real. The following explanation is offered:

Let it be hypothesised that the pressure fluctuations measured by a transducer in a wall are largely due to passage of pressure waves generated by upstream bursting events in the boundary layer. These cover many decades of frequency. In the non-dimensional form used in plotting mean square pressure amplitude there can be no difference between water and air because the burst mechanism must be similar in the two fluids. Let it be further hypothesised that a small percentage of the bursts occur immediately over the transducer and that the pressure produced by these is $\rho cv'$. Here ρ is the fluid density, c is its sound speed, and v' is the turbulent

fluctuating velocity normal to the wall associated with the burst. The large one-sided amplitude fluctuations in Fig. 9 may possibly be the results of bursts over the transducer. When this pressure is squared and averaged so that it can be plotted on the dimensionless ordinate scale of one of the spectral curves, it is obvious that the denominator will include the square of a Mach number; everything else will be similar in water and in air but at the usual test conditions the Mach number in water is considerably smaller than that in air. Hence, the mean square pressure amplitude would be expected to be somewhat larger in water than in air even if only a small percentage of the bursts occur directly over the transducer. Since bursting over the transducer occurs only infrequently, it must be most important in the low frequency region.

Taking a characteristic burst frequency as $\frac{1}{30} \frac{U_\infty}{\delta^*}$ [17, Fig. 42],

the corresponding abscissa scale on Figs. 1, 5, and 12 is $\omega \delta^* / U_\infty \approx 0.005$. This is far smaller than any recorded data but it would indicate that the hypothesized increase in pressure should be at least as pronounced at frequencies less than that at which the peak occurs as at the peak. The present data do not clearly substantiate this, but it must be remembered that low frequency data are hard to obtain. The Gershilov, et al data shown in Fig. 5 do seem to substantiate the expected effect.

The influence of roughness on pressure amplitude was shown in Fig. 14. There is a very clear increase in amplitude over the smooth surface case at low frequencies as well as a possible decrease in the dimensionless frequency of the peak. With Polyox added to the water, Fig. 16, the body with rough surface shows a decrease in pressure amplitude varying monotonically with drag reduction at low frequencies. It may be hypothesized that roughness produces additional pressure waves in the low frequency part of the spectrum, while polymer additive damps those waves. Whether the waves are produced by changes in the bursting rate or by direct production of turbulent eddies by the roughness particles, cannot be ascertained from these data.

Conclusions

Experimental measurements have been made of mean square pressure fluctuation amplitudes as a function of frequency in the boundary layer of an axi-symmetric body moving through water. Measurements were made in the zero pressure gradient portion of the body surface. Both smooth and grit-roughened surfaces were used and the body with rough surface moved through water containing polymer additive as well as through water without additive. Amplitudes and frequencies have been reduced to dimensionless form to permit comparison of one experiment with another as well as to facilitate comparison with work of others.

The following conclusions may be drawn:

1. The addition of roughness to a smooth surface increases the amplitude at the peak of the spectrum and at all lower frequencies for a body moving in water. It decreases the amplitude for higher frequencies beginning about a half decade above the peak.

2. Polymer additive in water causes the amplitude for the rough body to be reduced at the peak of the spectrum and at all lower frequencies. The reduction increases monotonically with drag reduction. There is no additional effect at high frequencies.

3. At high frequencies the spectra under all conditions--smooth and rough in water and rough in water with additive--fall at about 72dB/decade.

4. The peak of the spectrum in water is several decibels higher than the peak in air. This was attributed to the effect of turbulence bursts occurring directly over a transducer. Otherwise, the behavior is probably the same in water as in air.

The measurements were limited in many ways by the equipment that was available and the techniques that were used. It is believed that the above conclusions would be substantiated by any improvements in equipment or technique. However, better data are needed to confirm those conclusions and to extend them to answer other questions. Some specific needs are:

1. The conclusions regarding high frequency behavior are based on data taken with transducers whose face areas are too large compared to the boundary layer thickness. Smaller transducers should be designed and used. Also, the

transducer or electronic equipment used in data taking may have a high frequency resonance or cut-off point. Some of the data should be retaken with a transducer of a different make to check whether resonance has influenced any of the data points.

2. The measurements should be extended to other types of roughness and to a broader range of polymer concentrations or drag reduction.

3. Measurements at the lowest frequencies are uncertain because the test body has a short running time at terminal speed. These measurements can be improved by obtaining co-spectra from two closely spaced transducers; such measurements should be made. Analysis could also be improved by taking the ensemble average of many runs at terminal speed and analyzing the data with a sophisticated computer system. Equipment is just becoming available at this Laboratory to facilitate this kind of analysis.

4. Equipment needs to be developed to permit measuring and analyzing radiated noise from the boundary layer.

5. More detailed investigation should be undertaken of the basic boundary layer mechanism leading to pressure fluctuation and how this is influenced by roughness and polymer additive. The present work has been largely heuristic. Measurement of co-spectra, as already suggested, will contribute considerably to better understanding. Additional measurements correlating fluctuating pressures with fluctuating shears at the boundary and with fluctuating velocities will also be useful for this purpose.

List of References

- [1] Willmarth, W. W., "Pressure Fluctuations Beneath Turbulent Boundary Layers", Annual Review of Fluid Mechanics, 7:13-38 (1975).
- [2] Nisewanger, C. R. and Sperling, F. B., Flow Noise Inside Boundary Layers of Buoyancy-Propelled Test Vehicles, U.S. Naval Ordnance Test Station, NOTS TP3511, April 1965.
- [3] Blake, W. K., "Turbulent Boundary Layer Wall Pressure Fluctuations on Smooth and Rough Walls", Jour Fluid Mech, 44:637-660, (1970).
- [4] O'Keefe, E. J., Casarella, M. J., and DeMetz, F. C., Effect of Local Surface Roughness on Turbulent Boundary Layer-Wall Pressure Spectra and Transducer Burst Onset, U.S. NSRDC, Rpt 4702, Dec. 1975.
- [5] Greshilov, E. M., Evtushenko, A. V., and Lyamshev, L. M., "Hydrodynamic Noise and the Toms Effect", Soviet Physics, Acoustics, 21:247-251 (1975).
- [6] Killen, J. M., and Almo, J. A., The Influence of Drag Reducing Polymer Additives on Surface Pressure Fluctuations on Rough Surfaces, Project Report No. 119, St. Anthony Falls Hydraulic Laboratory, September 1971.
- [7] Millward, A., Turbulent Pressure Fluctuations in Water with Additives, Department of Aeronautics and Astronautics, University of Southampton, 1971.
- [8] Brady, J. F., An Experimental Study of the Vibration, Noise, and Drag of a Cylinder Rotating in Water and Certain Polymer Solutions, Ph.D. Thesis, University of Rhode Island, 1973.
- [9] Burton, T. E., The Connection Between Intermittent Turbulent Activity Near the Wall of a Turbulent Boundary Layer with Pressure Fluctuations at the Wall, Tech. Rpt. 70208-10, Department of Mechanical Engineering, Massachusetts Institute of Technology, June 1974.
- [10] Farabee, T. M. and Geib, F. E., Jr., Measurement of Boundary Layer Pressure Fields with an Array of Pressure Transducers in a Subsonic Flow, NSRDC Rpt 76-0031, March 1976.
- [11] Martin, N. C. and Leehey, P., "Low Wavenumber Wall Pressure Measurements Using a Rectangular Membrane as a Spatial Filter", Jour Sound & Vibration, 52:95-120 (1977).
- [12] Killen, J. M., A Buoyancy-Propelled-Test-Body Laboratory Facility, Project Report No. 149, St. Anthony Falls Hydraulic Laboratory, 1974.
- [13] Franz, G. J., "Flow Noise Measurements in Water", 72nd Meeting, Acoustical Society of America, Nov. 2-5, 1968.

List of References (cont.)

- [14] Pankhurst, R. C. and Holder, D. W., Wind-Tunnel Technique, Pitman & Sons, London, p. 340, 1952.
- [15] Granville, P. S., The Calculation of the Viscous Drag of Bodies of Revolution, David Taylor Model Basin, Rpt. 849 (1953).
- [16] Sirmalis, J. E., A Study of the Drag Characteristics and Polymer Diffusion in the Boundary of an Axisymmetric Body, Naval Underwater Systems Center, Tech. Rpt 4860, 1976.
- [17] Wilmarth, W. W., "Structure of Turbulence in the Boundary Layer", Advances in Applied Mechanics, 15:159-254, 1975.

List of Figures

1. Wall pressure spectrum, smooth wall, after Blake [3].
2. Wall pressure spectra, smooth and rough wall comparison, after Blake [3].
3. Wall pressure spectrum, rough walls. Inner variable scaling, after Blake [3].
4. Wall pressure spectrum rough walls. Inner variable scaling, after Blake [3].
5. Wall pressure spectra, smooth wall in water.
6. Spectra in channel with water flowing [5].
7. Sketch of standpipe installed in Laboratory building.
8. Sketch of test body (dimensions in cm).
9. Typical body surface pressure data. Body with rough surface in water. Drag - 342.9 N.
10. Typical pressure data at fixed position in standpipe. Body with rough surface in water. Drag - 222.8 N.
 - a) Small pressure amplification
 - b) Larger pressure amplification
11. Photograph of Roughness (scale in mm).
12. Wall pressure spectrum in water, smooth wall. Outer variable scaling.
13. Wall pressure spectrum in water, smooth wall. Inner variable scaling.
14. Wall pressure spectrum in water, rough wall. Inner variable scaling.
15. Wall pressure spectrum in water, rough wall. Inner variable roughness scaling.
16. Wall pressure spectrum in water with Polyox, rough wall. Inner variable scaling.

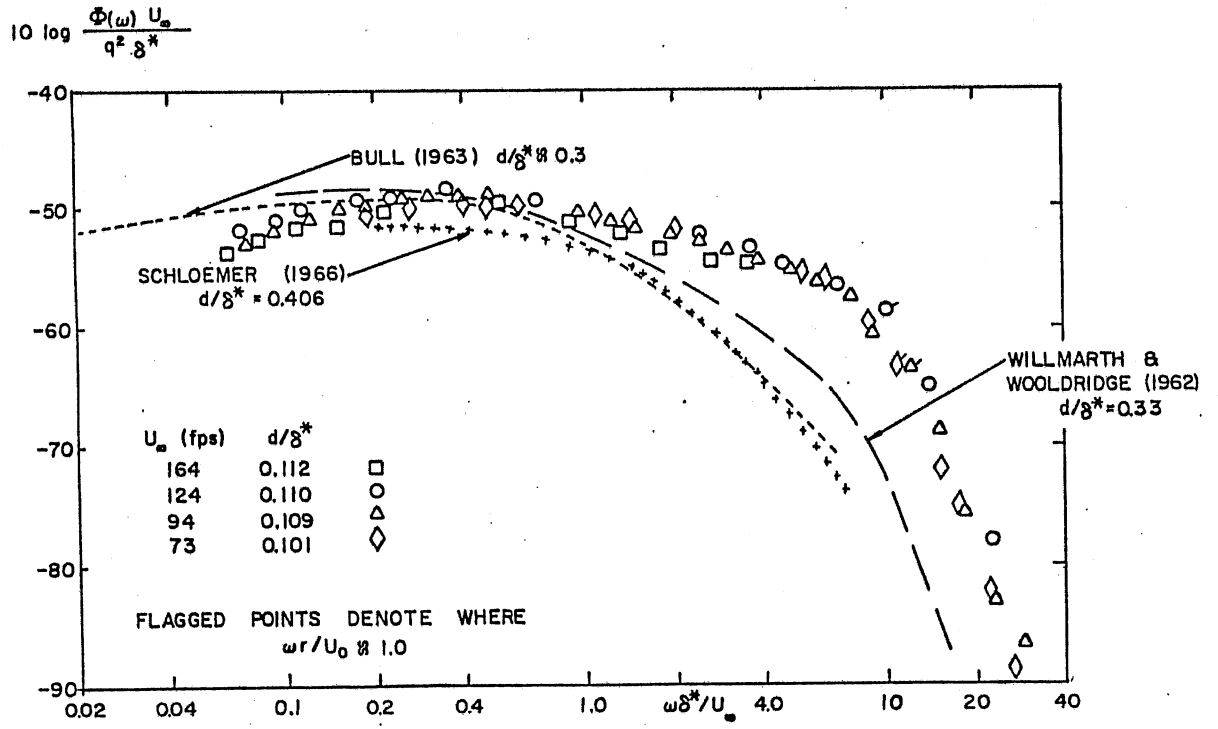


Fig. 1. Wall pressure spectrum, smooth wall, after Blake [3]

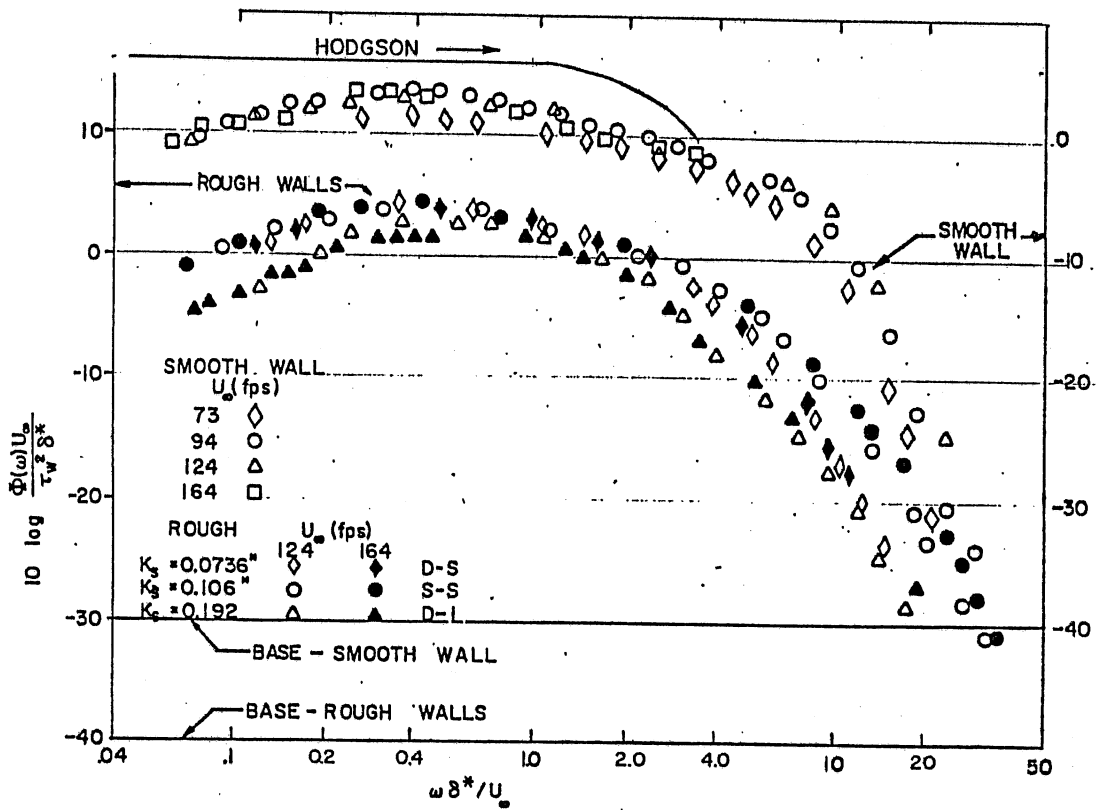


Fig. 2. Wall pressure spectra, smooth and rough wall comparison, after Blake [3]

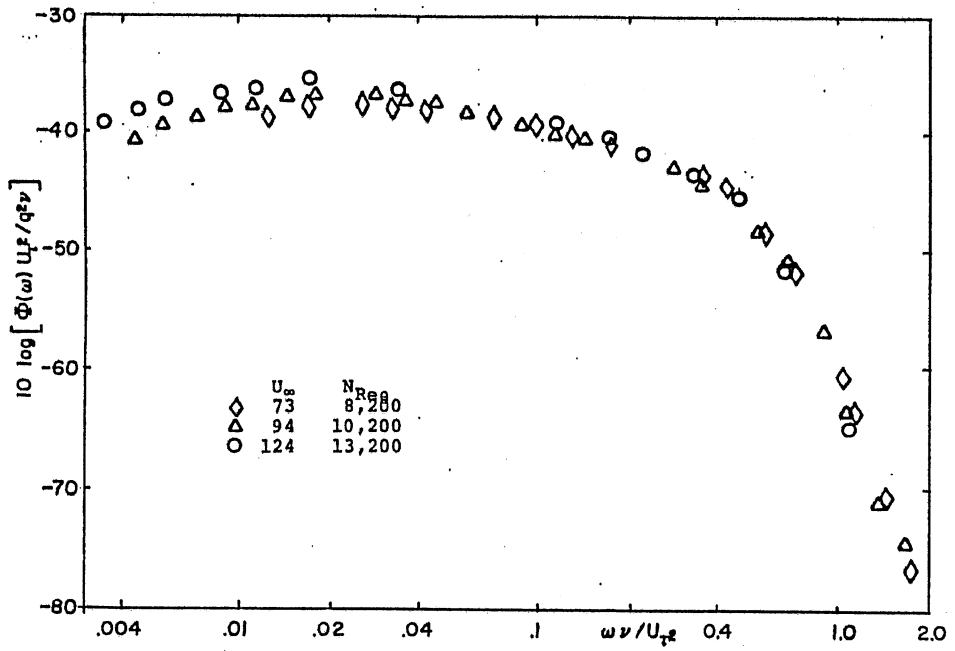


Fig. 3. Wall pressure spectrum, smooth wall inner variable scaling, after Blake [3]

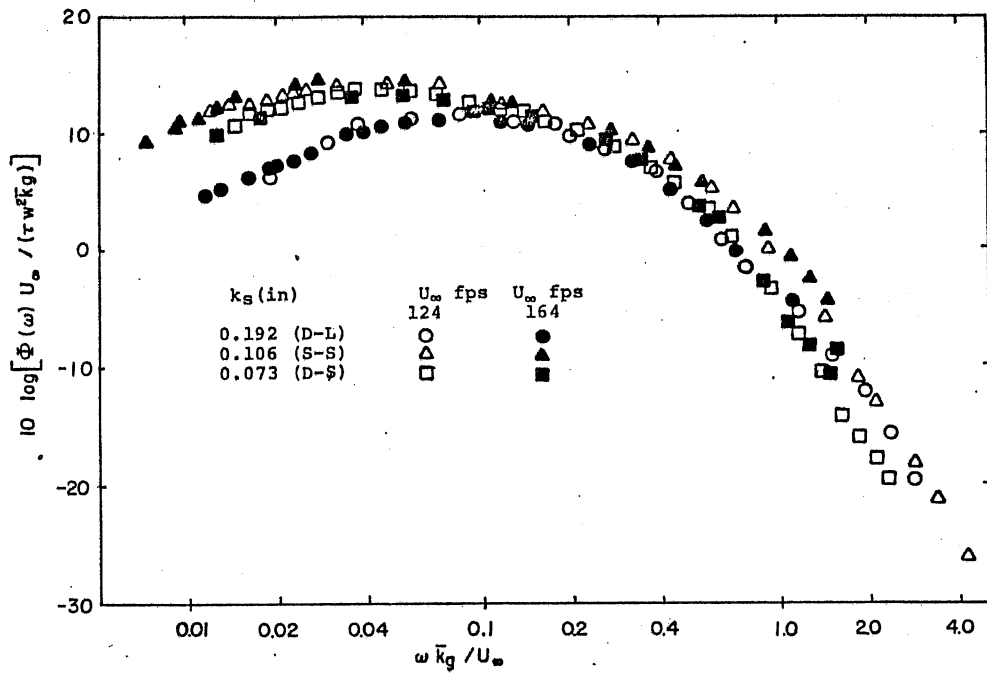


Fig. 4. Wall pressure spectrum, rough walls, inner variable scaling, after Blake [3]

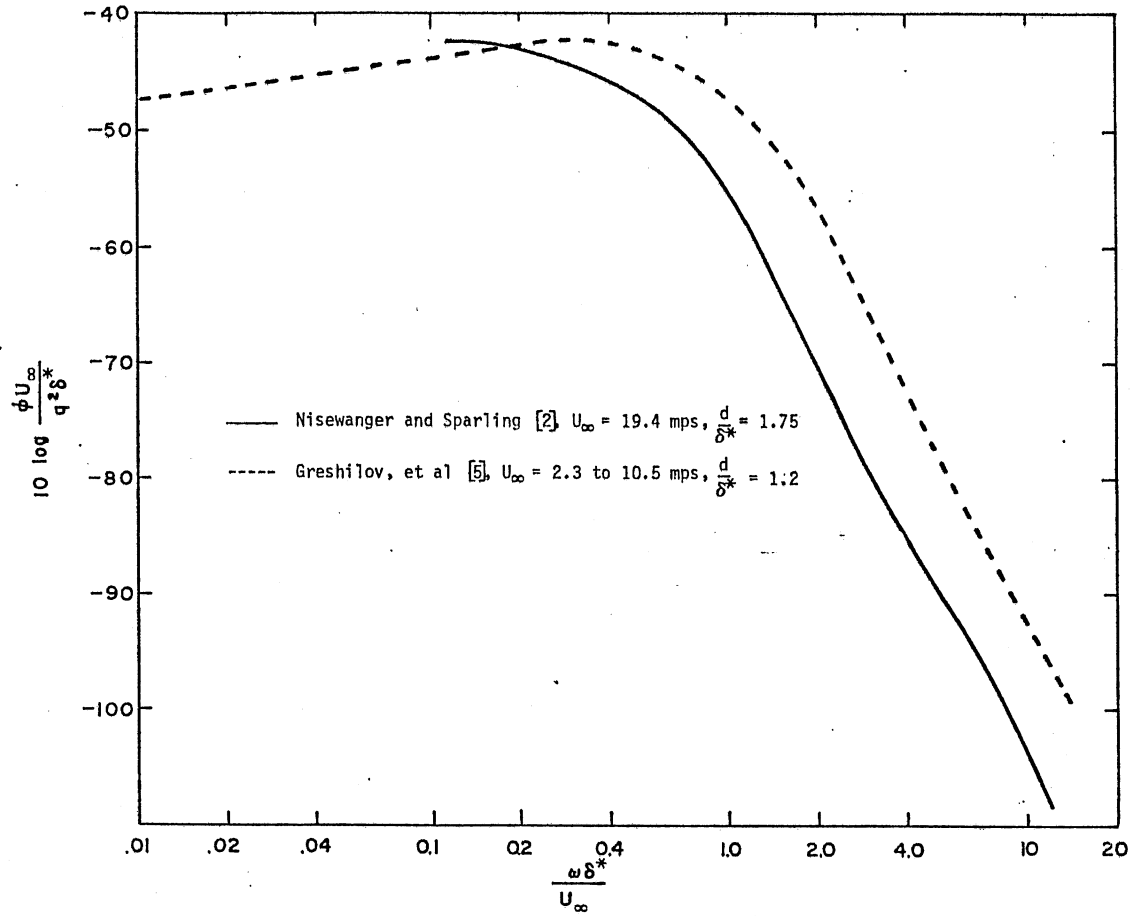


Fig. 5. Wall pressure spectra, smooth wall in water.

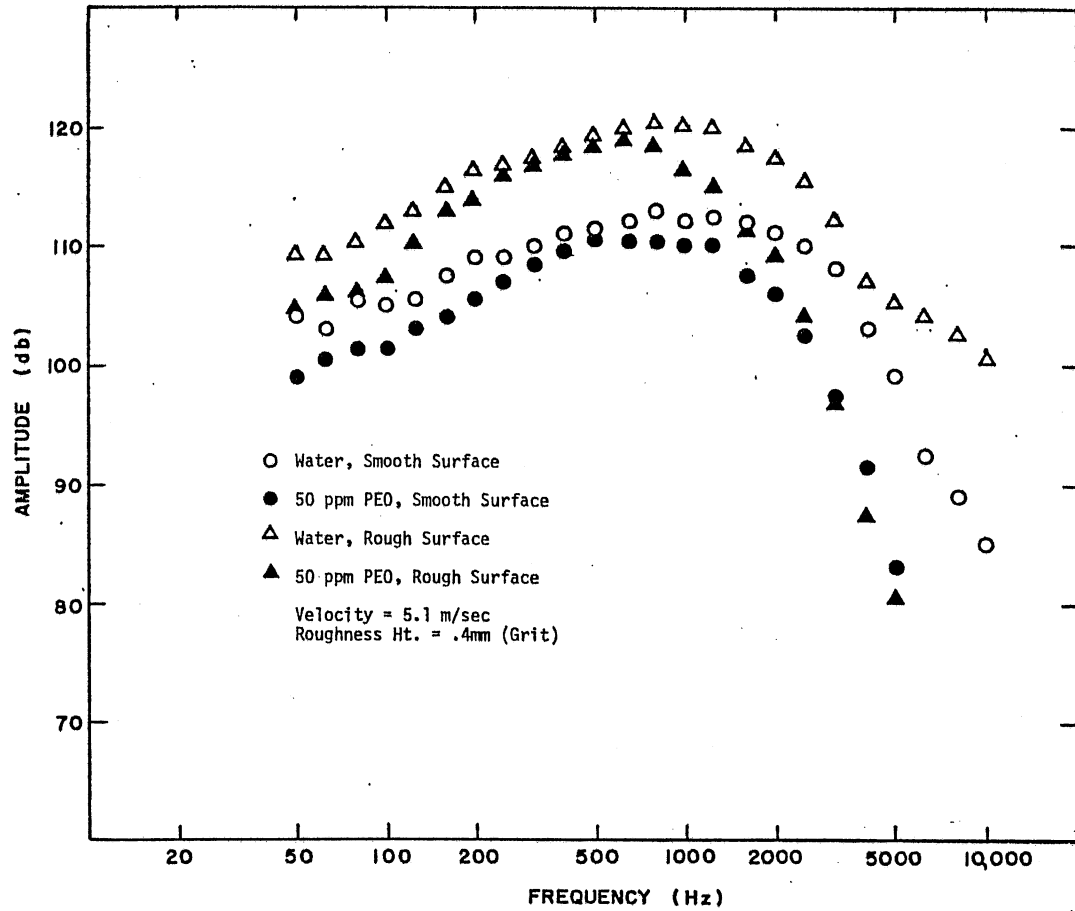


Fig. 6. Spectra in channel with water flowing [5]

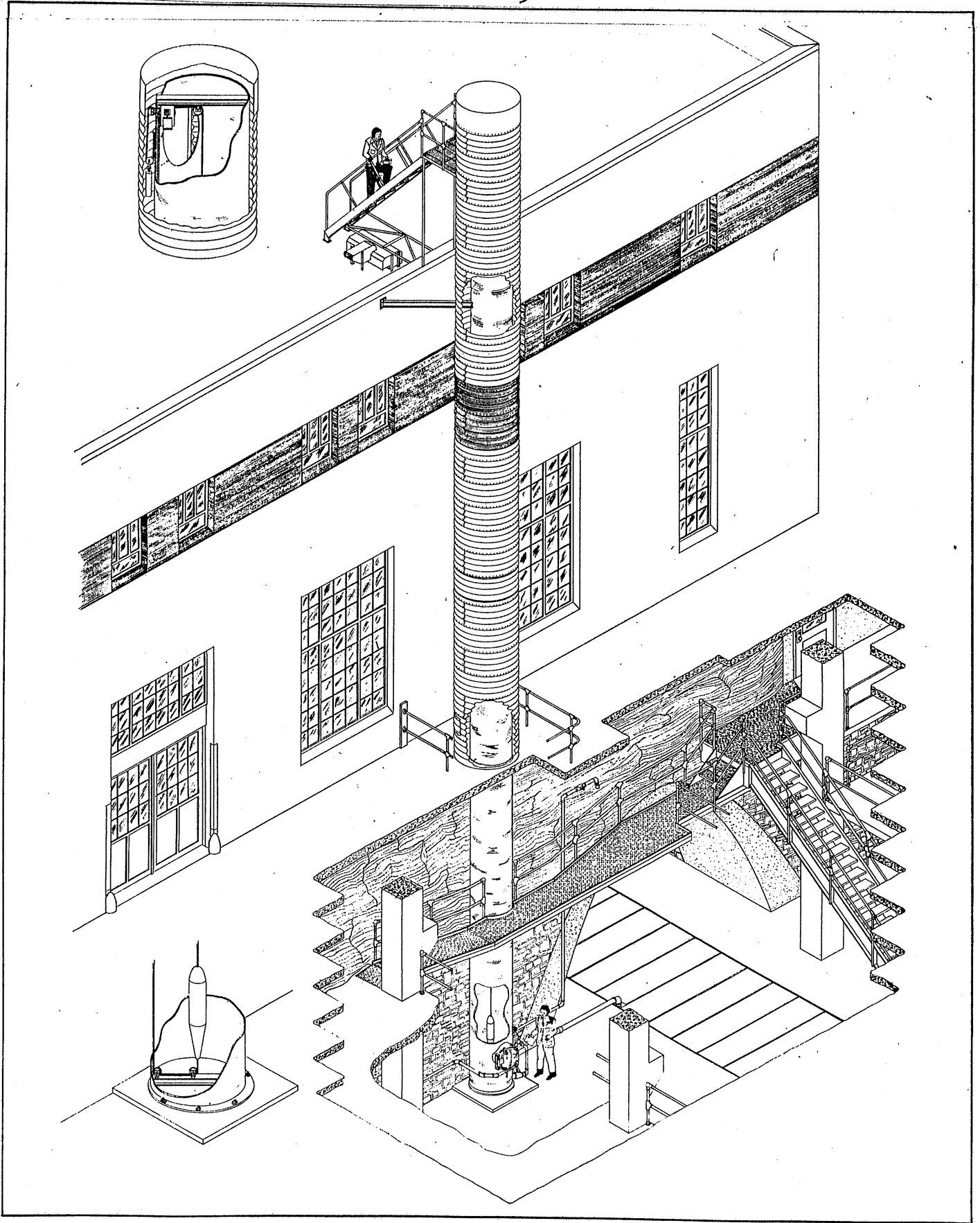
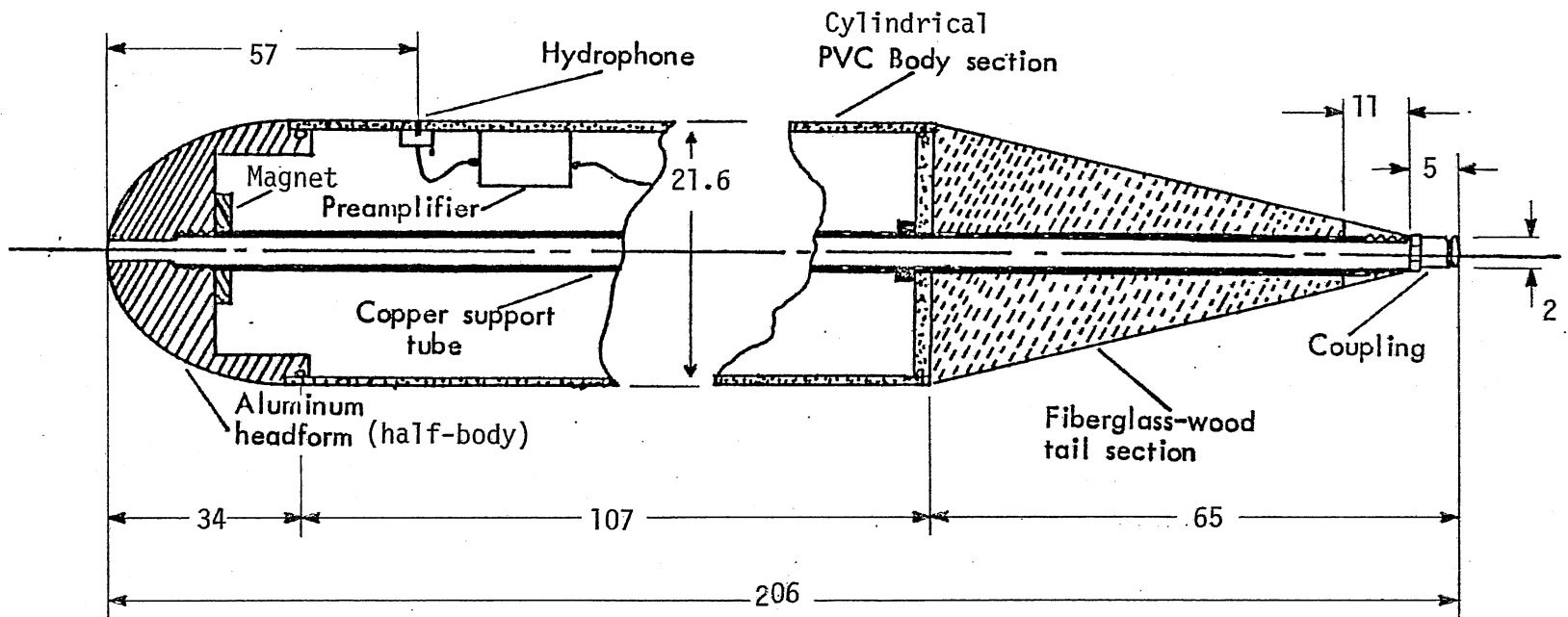


Fig. 7 - Sketch of standpipe installed in laboratory building



Surface Area = 1.24 m²

Fig. 8. Sketch of test body (dimensions in cm).

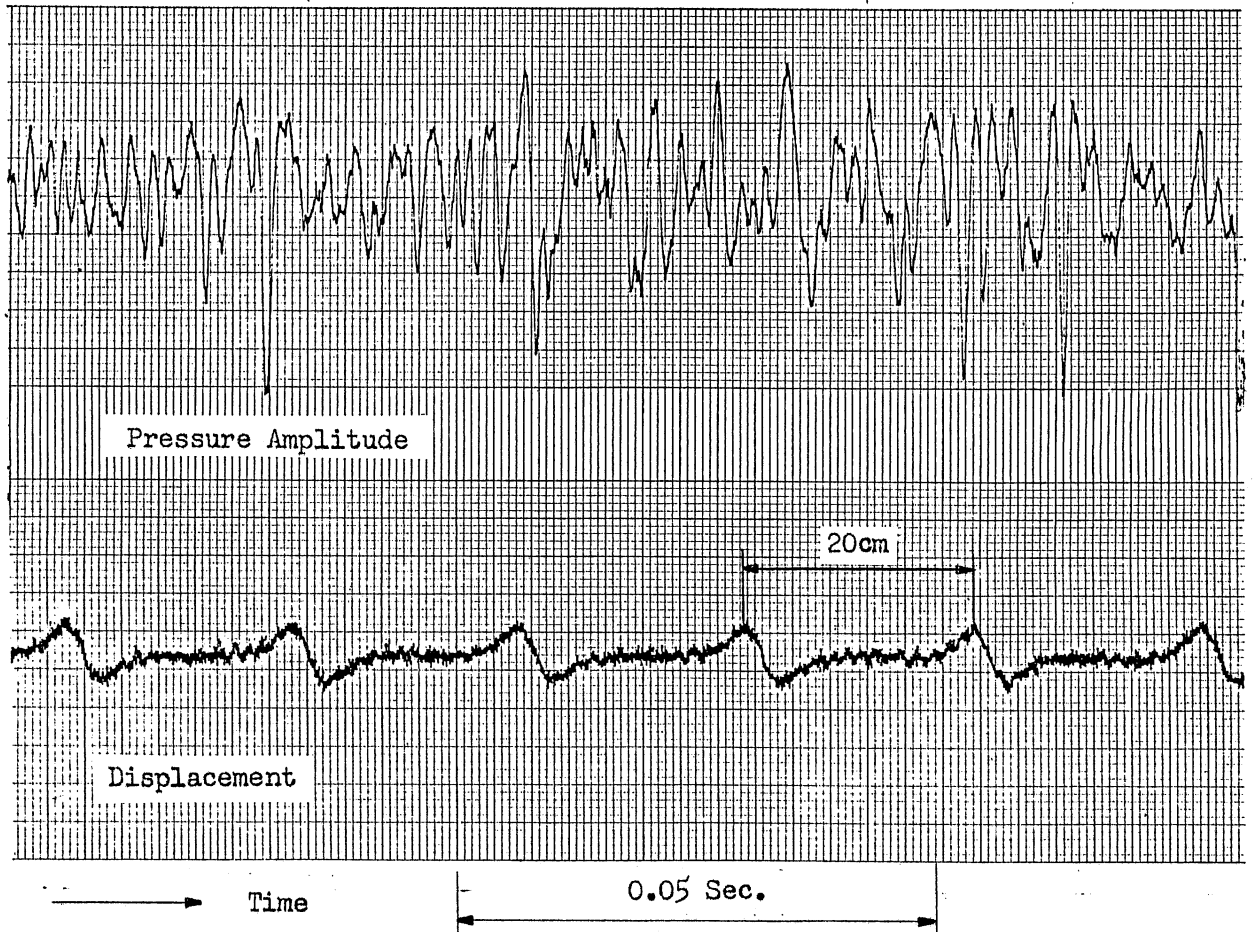


Fig. 9. Typical body surface pressure data. Body with rough surface in water. Drag = 342.9 N.

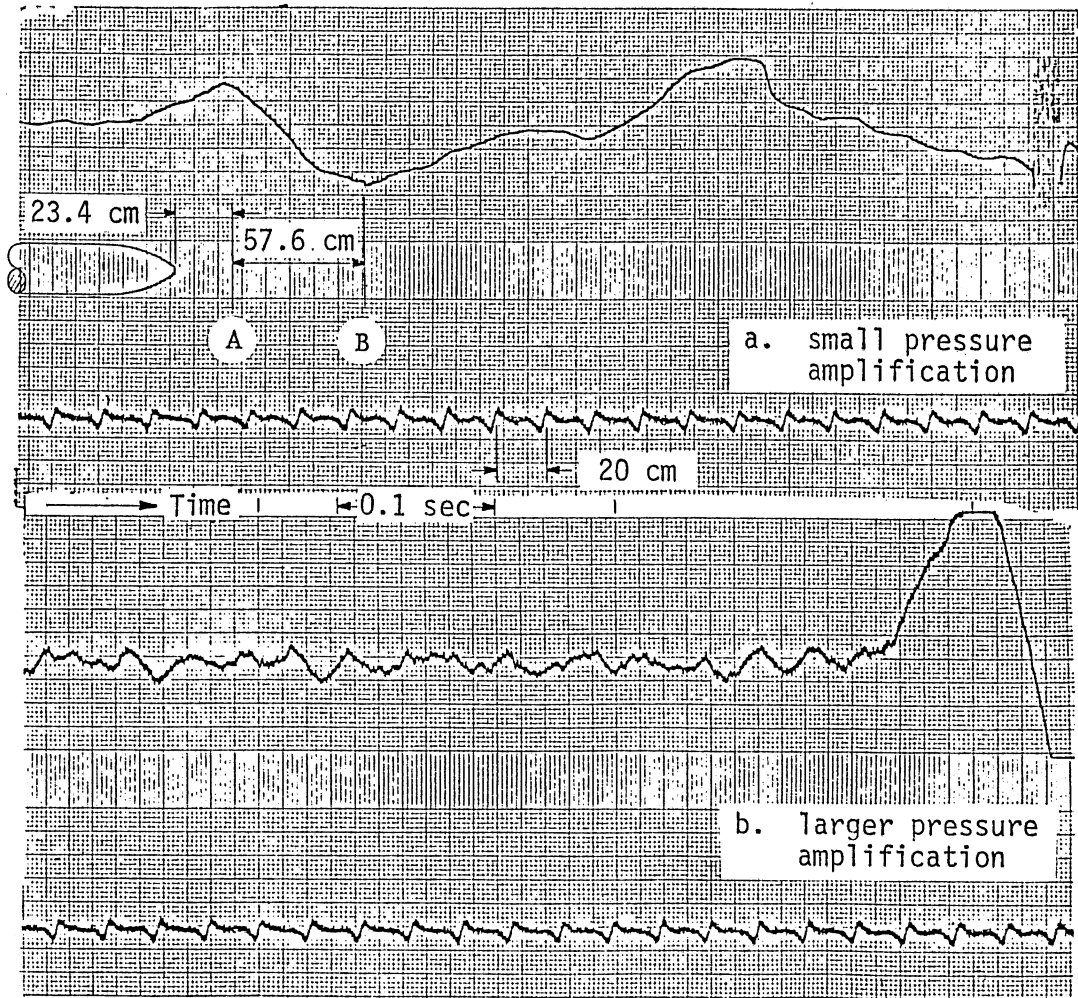


Fig. 10. Typical pressure data at fixed position in standpipe. Body with rough surface. Drag = 228.8 N.

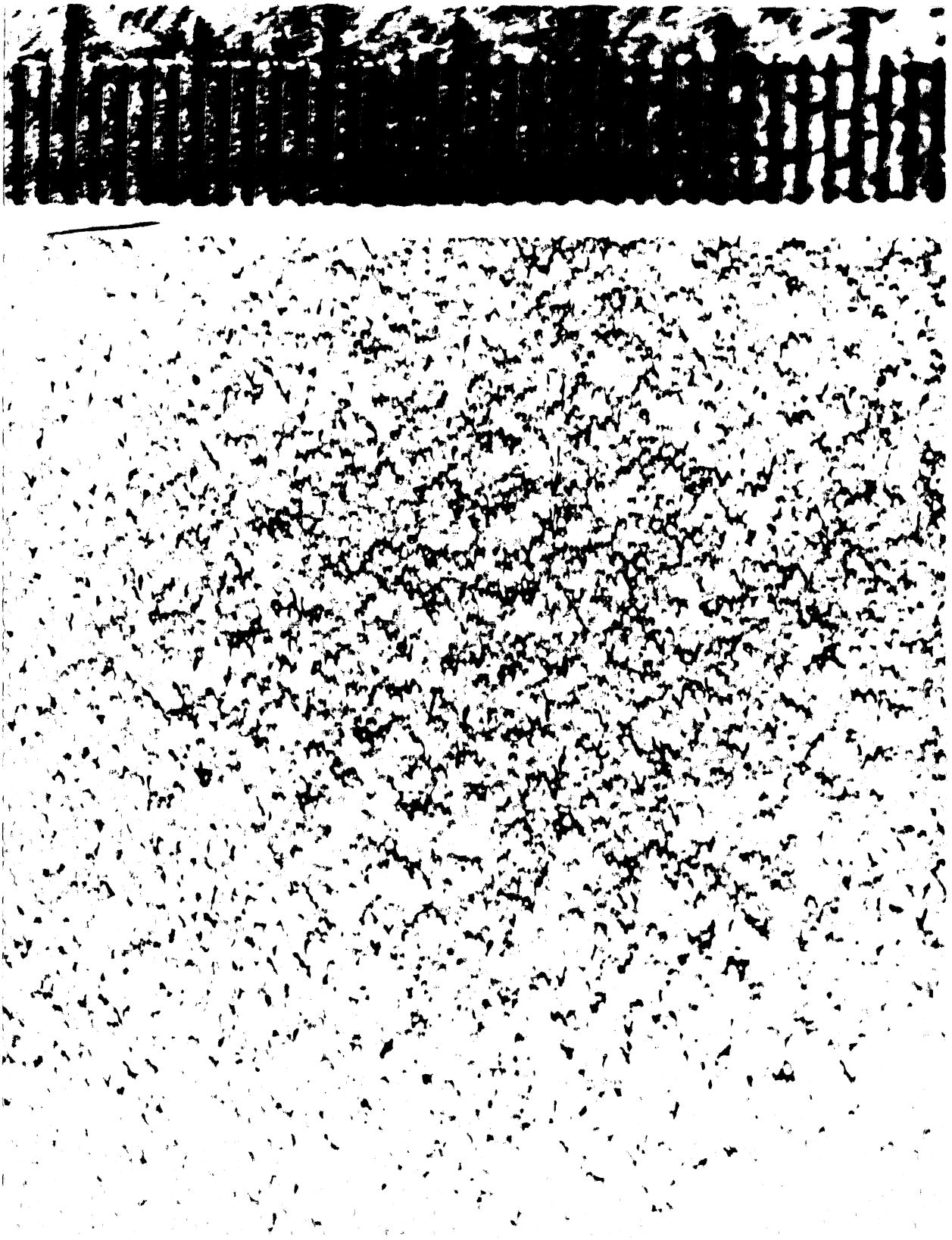


Fig. 11. Photograph of Roughness (scale in mm).

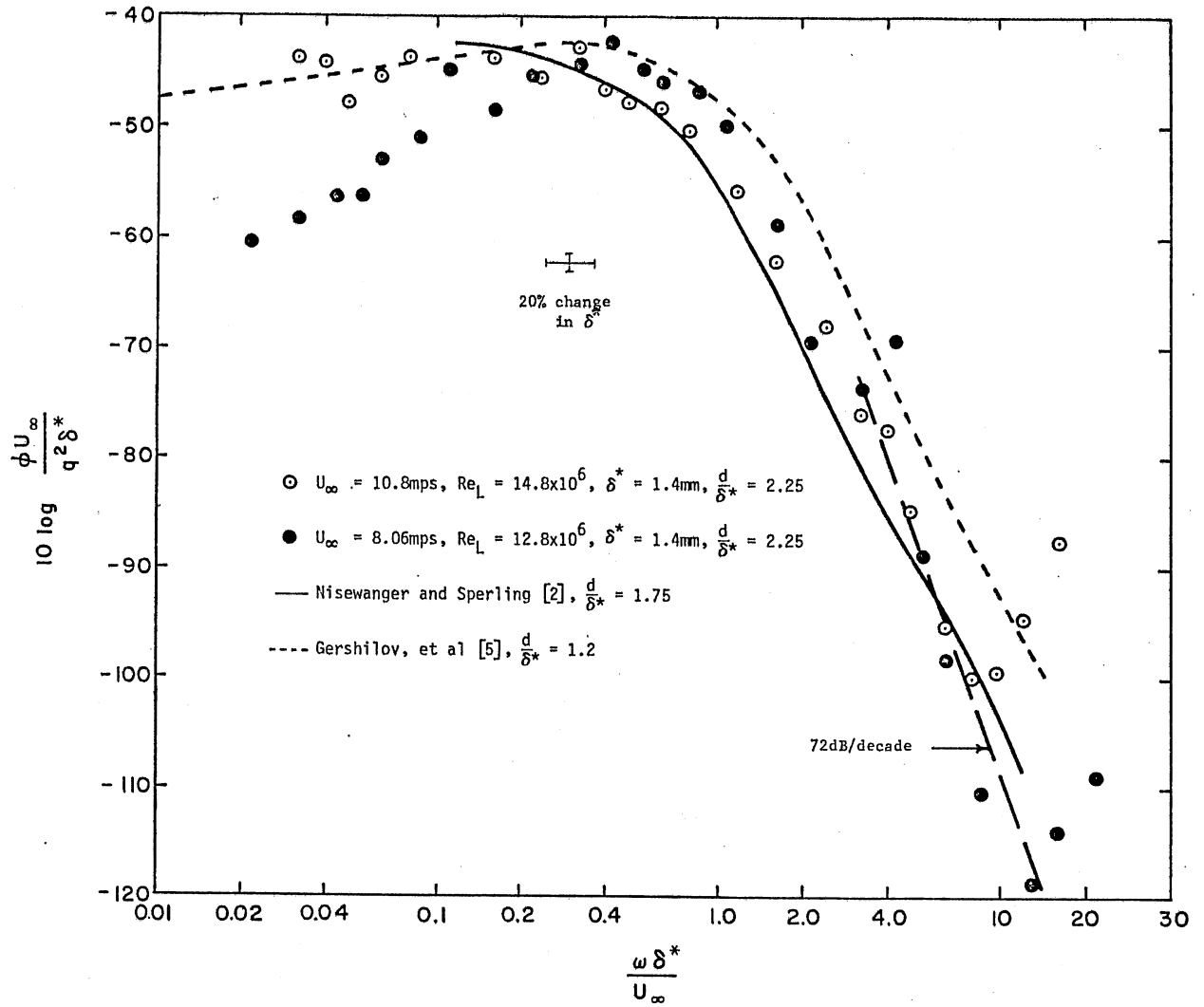


Fig. 12. Wall pressure spectrum in water, smooth wall. Outer variable scaling.

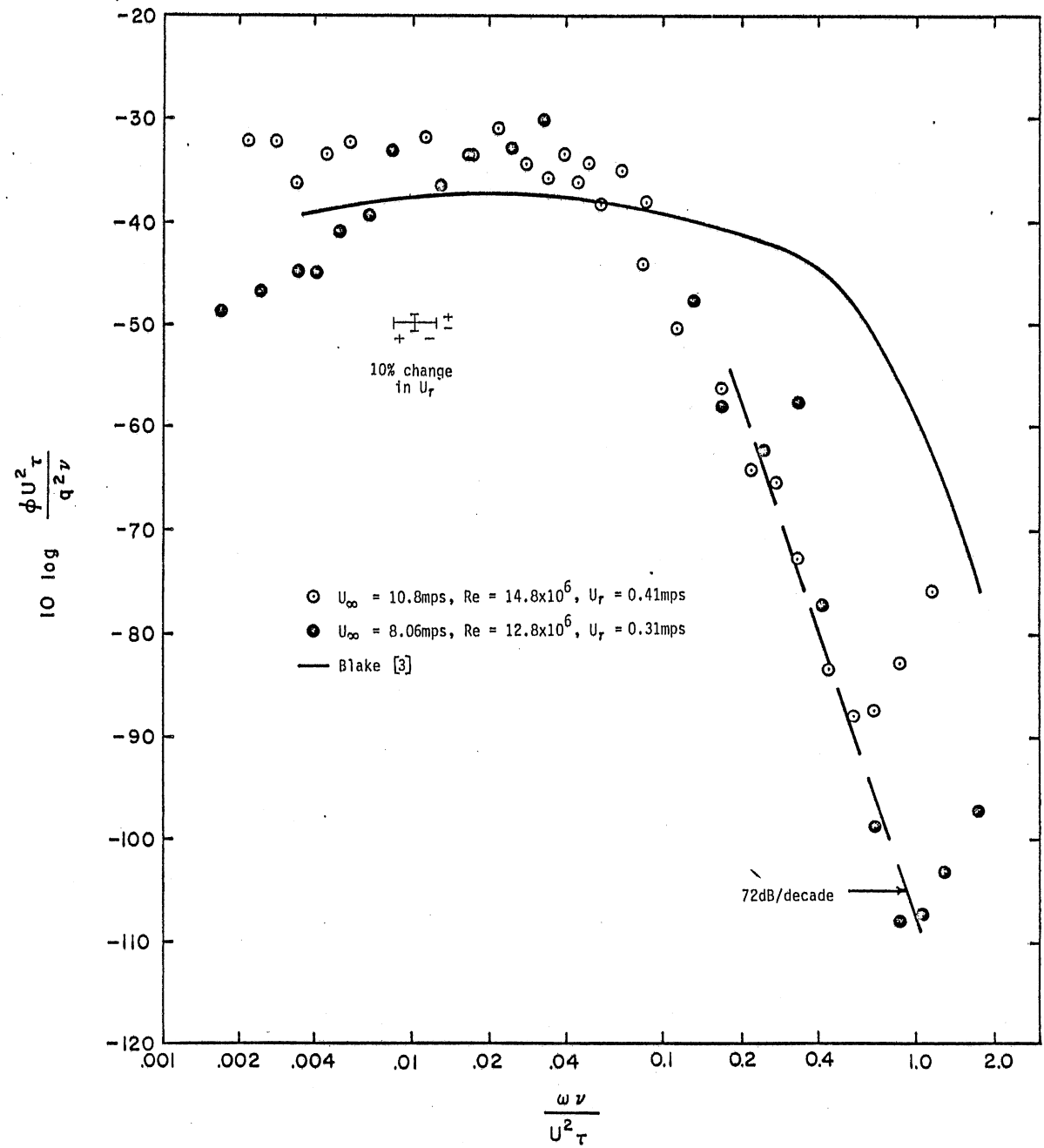


Fig. 13. Wall pressure spectrum in water, smooth wall. Inner variable scaling.

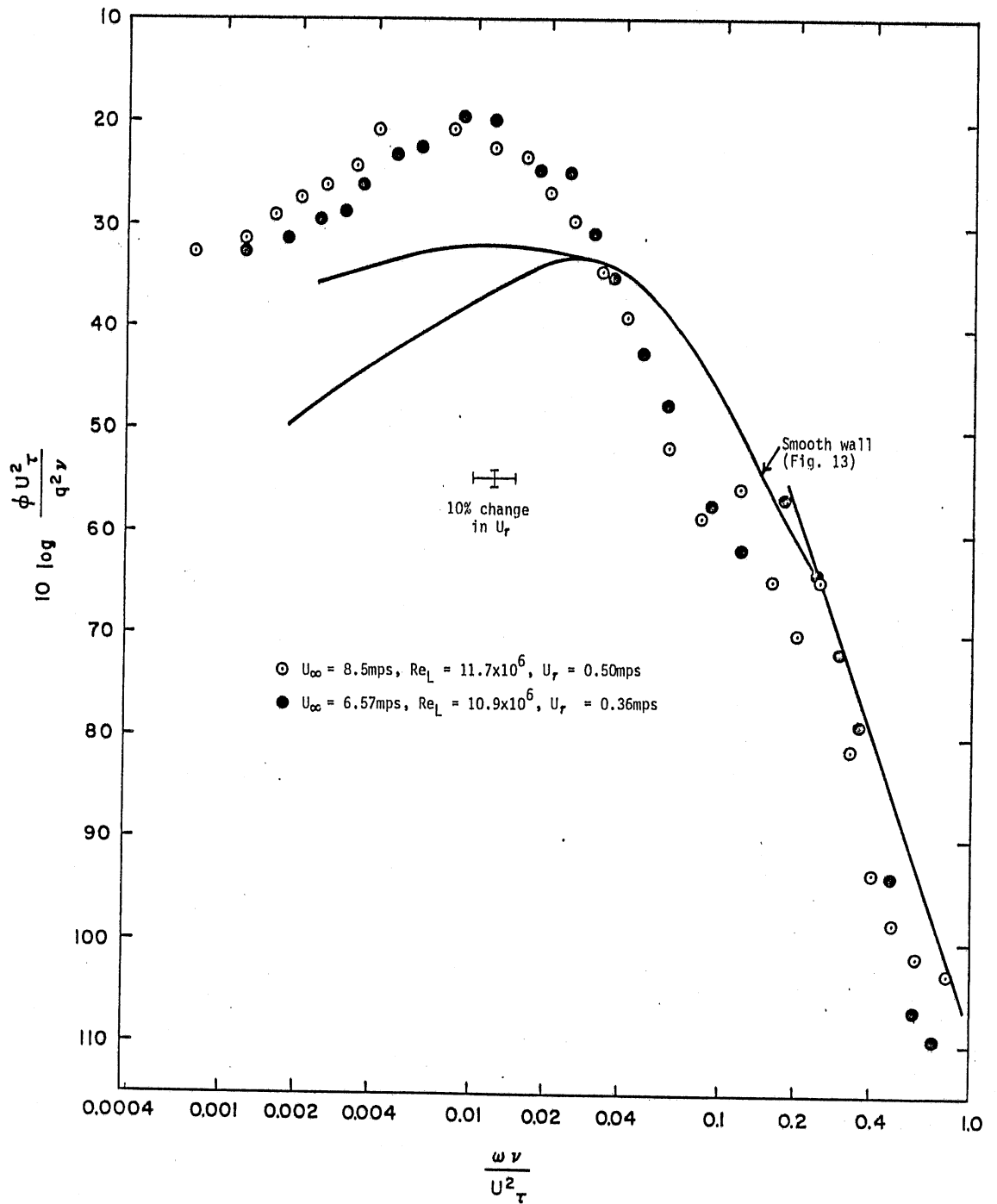


Fig. 14. Wall pressure spectrum in water, rough wall. Inner variable scaling.

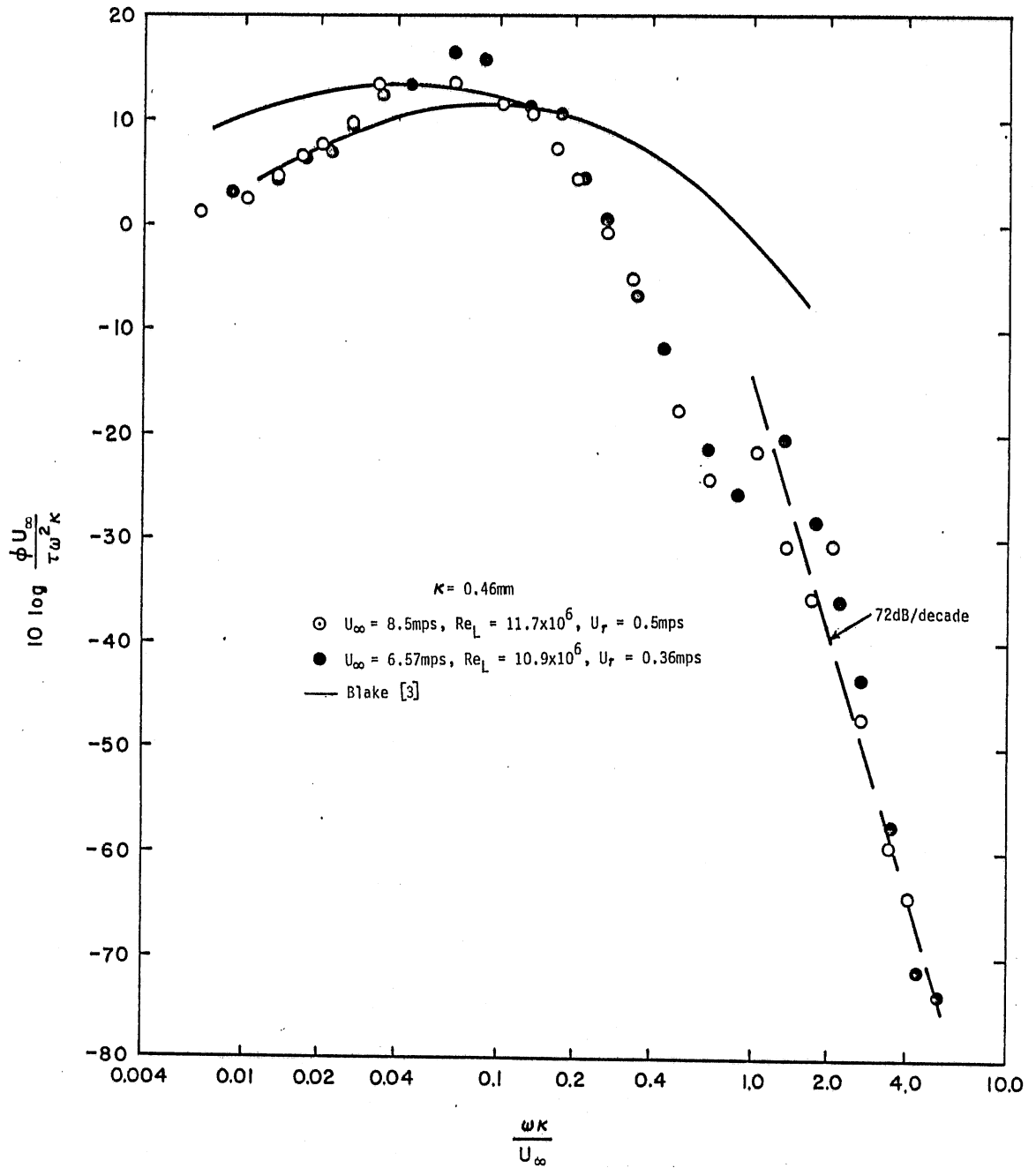


Fig. 15. Wall pressure spectrum in water, rough wall. Inner variable roughness scaling.

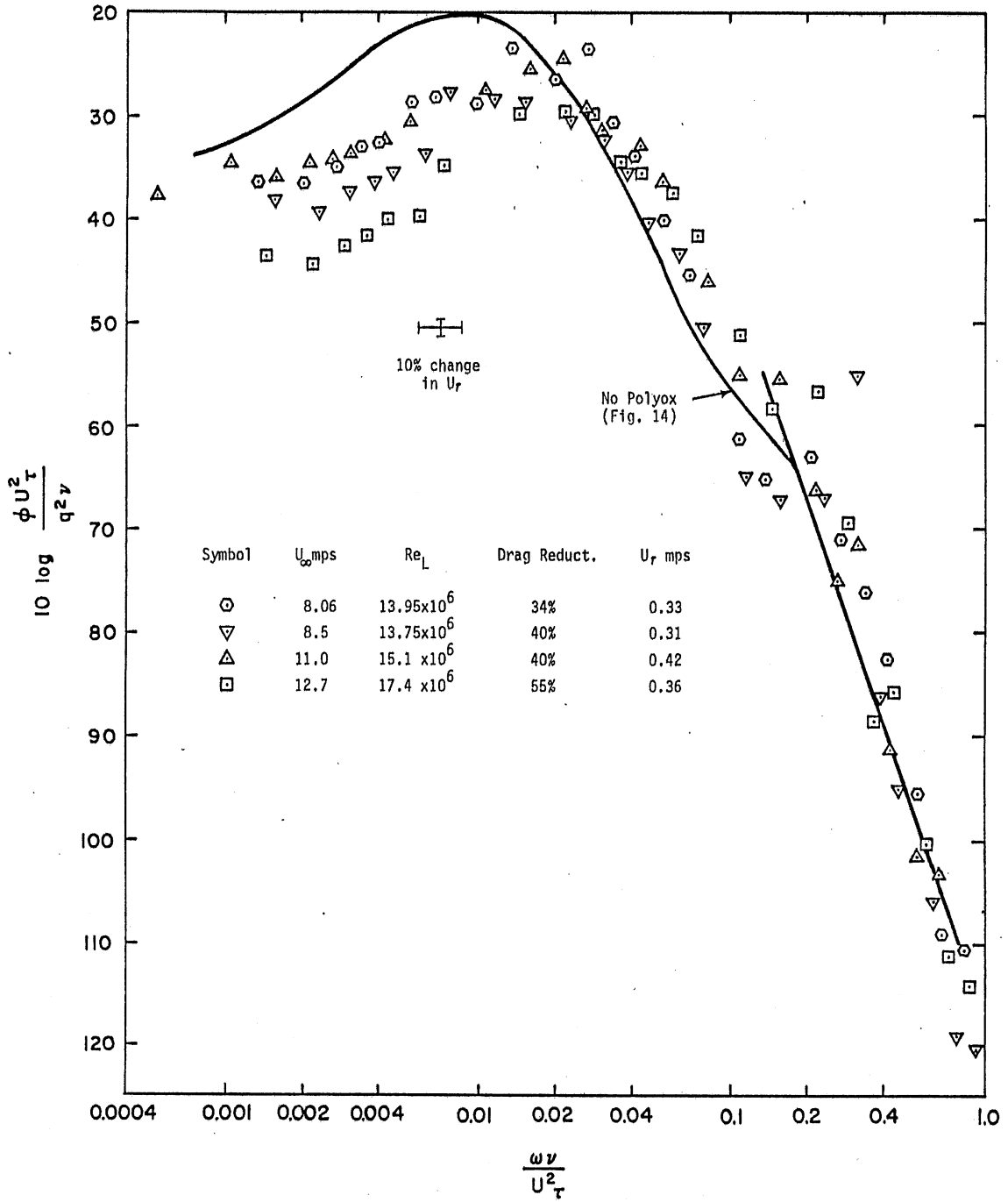


Fig. 16. Wall pressure spectrum in water with polyox, rough wall. Inner variable scaling.

REPORT DOCUMENTATION PAGE		READ INSTRUCTIONS BEFORE COMPLETING FORM
1. REPORT NUMBER Project Report No. 172	2. GOVT ACCESSION NO.	3. RECIPIENT'S CATALOG NUMBER
4. TITLE (and Subtitle) AN EXPERIMENTAL INVESTIGATION OF THE EFFECT OF DRAG REDUCING POLYMER ADDITIVES ON SURFACE PRESSURE FLUCTUATIONS ON BODIES OF REVOLUTION WITH ROUGH SURFACES MOVING THROUGH WATER		5. TYPE OF REPORT & PERIOD COVERED Final May 1, 1977 - December 31, 1979
		6. PERFORMING ORG. REPORT NUMBER Project Report No. 172
7. AUTHOR(s) Edward Silberman		8. CONTRACT OR GRANT NUMBER(s) N00014-77-0356
9. PERFORMING ORGANIZATION NAME AND ADDRESS St. Anthony Falls Hydraulic Laboratory Mississippi River at 3rd Ave. S.E. Minneapolis, Minnesota 55414		10. PROGRAM ELEMENT, PROJECT, TASK AREA & WORK UNIT NUMBERS 61153N, R02301, SRO230101, #1898
11. CONTROLLING OFFICE NAME AND ADDRESS David W. Taylor Naval Ship Research and Develop- ment Center (DTNSRDC) Ship Performance Dept. (Code 1505) Bethesda, Md. 20884		12. REPORT DATE May 1978
		13. NUMBER OF PAGES 36
14. MONITORING AGENCY NAME & ADDRESS (if different from Controlling Office) Same		15. SECURITY CLASS. (of this report) Unclassified
		15a. DECLASSIFICATION/DOWNGRADING SCHEDULE
16. DISTRIBUTION STATEMENT (of this Report) Approved for public release; distribution unlimited		
17. DISTRIBUTION STATEMENT (of the abstract entered in Block 20, if different from Report)		
18. SUPPLEMENTARY NOTES		
19. KEY WORDS (Continue on reverse side if necessary and identify by block number) Boundary Layer, Pressure Fluctuations, Noise, Polymer Additive, Roughness		
20. ABSTRACT (Continue on reverse side if necessary and identify by block number) A sound detector in the surface of a moving body receives not only sound signals radiated from a distant source but also detects pressure fluctuations originating in the turbulent boundary layer of the fluid surrounding the body. The purpose of the present work was to assess the magnitude of the surface pressure fluctuations on a body moving in water and in water with polymer additive under nearly zero pressure gradient conditions. Measurements were made using a single transducer in the surface of an axi-symmetric body. Both smooth and grit-roughened surfaces were used. Mean square pressure fluctuation		

#20

amplitudes were measured as a function of frequency, non-dimensionalized, plotted, and compared with results obtained by others in both water and air.

It was concluded that the addition of roughness to a smooth surface increases the amplitude at the peak of the spectrum and at all lower frequencies. Polymer additive in the water has just the opposite effect on a rough-surfaced body, decreasing the amplitude at the peak and at all lower frequencies, the reduction increasing monotonically with drag reduction. There was little or no effect at high frequencies attributable to either roughness or polymer additive, but it must be noted that the transducer used was too large to obtain a true measure of amplitude at the highest frequencies. The peak of the spectrum in water appears to have a somewhat higher amplitude than it does in air.